Spitzer Space Telescope Observations of G Dwarfs in the Pleiades: Circumstellar Debris Disks at 100 Myr Age

M. Silverstone – University of Arizona
et al.

Citation of published version:

Stauffer, J., et al. (2005): *Spitzer Space Telescope* Observations of G Dwarfs in the Pleiades: Circumstellar Debris Disks at 100 Myr Age. *The Astronomical Journal*, 130(4).
DOI: https://doi.org/10.1086/444420

The Astronomical Journal, 130:1834–1844, 2005 October

SPITZER SPACE TELESCOPE OBSERVATIONS OF G DWARFS IN THE PLEIADES: CIRCUMSTELLAR DEBRIS DISKS AT 100 Myr AGE[1,2]

John R. Stauffer
Spitzer Science Center, California Institute of Technology, Mail Code 314-6, 1200 East California Boulevard, Pasadena, CA 91125; stauffer@ipac.caltech.edu

Luisa M. Rebull
Spitzer Science Center, California Institute of Technology, Mail Code 220-6, 1200 East California Boulevard, Pasadena, CA 91125

John Carpenter and Lynne Hillenbrand
Astronomy Department, California Institute of Technology, 1200 East California Boulevard, Pasadena, CA 91125

Dana Backman
SOFIA and SETI Institute, MS 211-3, NASA Ames Research Center, Mountain View, CA 94035-1000

Michael Meyer, Jinyoung Serena Kim, Murray Silverstone, and Erick Young
Steward Observatory, University of Arizona, 933 North Cherry Avenue, Tucson, AZ 85726

Dean C. Hines
Space Science Institute, 4750 Walnut Street, Suite 205, Boulder, CO 80301

David R. Soderblom
Space Telescope Science Institute, 3700 San Martin Drive, Baltimore, MD 21218

Eric Mamajek
Center for Astrophysics, 60 Garden Street, Cambridge, MA 02138

Patrick Morris
Infrared Processing and Analysis Center, California Institute of Technology, Mail Code 314-6, Pasadena, CA 91125

Jeroen Bouwman
Max-Planck-Institut für Astronomie, Koenigstuhl 17, Heidelberg D-69117, Germany

and

Stephen E. Strom
National Optical Astronomy Observatory, 950 North Cherry Avenue, Tucson, AZ 85719
Received 2005 June 2; accepted 2005 June 28

ABSTRACT

Fluxes and upper limits in the wavelength range from 3.6 to 70 μm from the *Spitzer Space Telescope* are provided for 20 solar-mass Pleiades members. One of these stars shows a probable mid-IR excess, and two others have possible excesses, presumably due to circumstellar debris disks. For the star with the largest, most secure excess flux at MIPS (Multiband Imaging Photometer for *Spitzer*) wavelengths, HII 1101, we derive $\log (L_{\rm dust}/L_*) \sim -3.8$ and an estimated debris disk mass of $4.2 \times 10^{-5}\ M_\bullet$ for an assumed uniform dust grain size of 10 μm. If the stars with detected excesses are interpreted as stars with relatively recent, large collisional events producing a transient excess of small dust particles, the frequency of such disk transients is $\sim$10% for our $\sim$100 Myr, Pleiades G dwarf sample. For the stars without detected 24–70 μm excesses, the upper limits to their fluxes correspond to approximate 3 σ upper limits to their disk masses of $6 \times 10^{-6}\ M_\bullet$ using the MIPS 24 μm upper limit or $2 \times 10^{-4}\ M_\bullet$ using the MIPS 70 μm limit. These upper limit disk masses (for "warm" and "cold" dust, respectively) are roughly consistent with, but somewhat lower than, predictions of a heuristic model for the evolution of an "average" solar-mass star's debris disk based on extrapolation backward in time from current properties of the Sun's Kuiper Belt.

Key words: open clusters and associations: individual (Pleiades) — stars: low-mass, brown dwarfs

1. INTRODUCTION

The Formation and Evolution of Planetary Systems (FEPS) *Spitzer Space Telescope* Legacy program is observing a sample of 328 relatively nearby low-mass stars with masses in the range $0.8 < M/M_\odot < 1.5$ and with a range of ages from 3 Myr to about 3 Gyr (Meyer et al. 2004). The goal of the program is to determine empirically the ubiquity and evolution of circumstellar dust disks around approximately solar-mass stars and hence to put constraints on the frequency and timescale for the formation of planets around such stars. All the program stars are being observed with all three of *Spitzer*'s instruments: IRAC (3.6, 4.5, and 8.0 μm) in order to help define the photospheric flux at short wavelengths and to look for "hot" dust analogous to the solar system's inner zodiacal dust, IRS (5–38 μm low-resolution spectra) in order to place constraints on the particle size and

[1] This work is based (in part) on observations made with the *Spitzer Space Telescope*, which is operated by the Jet Propulsion Laboratory, California Institute of Technology, under NASA contract 1407.

[2] This publication makes use of data products from the Two Micron All Sky Survey, which is a joint project of the University of Massachusetts and the Infrared Processing and Analysis Center, California Institute of Technology, funded by the National Aeronautics and Space Administration and the National Science Foundation.

mineralogy, and MIPS (24 and 70 μm, and in some cases 160 μm) in order to place limits on the presence of cool dust around these stars.

Most of the FEPS sample of stars are field dwarfs whose ages are estimated from a variety of somewhat indirect techniques. However, the FEPS sample also includes about 120 stars in several open clusters or associations, chosen to sample a range in age from a few to about 600 Myr. These stars have the advantage that they have much better determined ages than the field stars; however, they are also, on average, considerably farther away than the other stars in the FEPS sample, and therefore, the ability to detect disks with *Spitzer* data is diminished. The clusters included in the FEPS target list are the Hyades (age $\sim$600 Myr), the Pleiades (age $\sim$100 Myr; Meynet et al. 1993), Alpha Persei (age $\sim$75 Myr; Ventura et al. 1998; Stauffer et al. 1999), IC 2602 (age $\sim$45 Myr; Mermilliod 1981; Stauffer et al. 1997; Barrado y Navascués et al. 2004), and the Sco-Cen association (age $\sim$5–17 Myr; Preibisch et al. 2001; Mamajek et al. 2002). In this paper we describe the *Spitzer* observations we have obtained of the Pleiades stars that are included in the FEPS program. Note that a *Spitzer* guaranteed time program led by J. Muzerolle has obtained *Spitzer* data for higher mass stars in the Pleiades. Those data will be reported in a separate paper.

Observations of the low-mass stars in young open clusters show that those stars arrive on the main sequence with a wide range of rotational velocities. Half or more arrive on the main sequence with low rotational velocities ($v \sin i < 20$ km s^{-1}); the remainder arrive on the main sequence as rapid rotators, with rotational velocities up to almost 200 km s^{-1}. A commonly proposed model for explaining the wide spread in zero-age main sequence (ZAMS) rotational velocity is that angular momentum is transferred to circumstellar disks during pre-main-sequence (PMS) evolution via magnetic fields (''disk locking''), and hence the stars that are slowly rotating upon arrival on the ZAMS are those that had the longest lived PMS accretion disks (Bouvier et al. 1993). If one further assumes that stars with long-lived accretion disks also are likely to have longer lived or more massive debris disks, then there should be a correlation between rotational velocity and mid-IR excess for young low-mass stars. An age of order 100 Myr (i.e., the Pleiades age) should be ideal for looking for this correlation, because main-sequence angular momentum loss from winds will not yet have significantly affected the rotational velocities, and the debris disks should be relatively massive and bright in the mid-IR compared to such disks surrounding older main-sequence stars. The Pleiades low-mass stars exhibit the large rotational velocity range that is desired for this experiment (van Leeuwen et al. 1986; Stauffer & Hartmann 1987; Queloz et al. 1998); *Spitzer* may be able to provide the mid-IR data necessary to link these rotational velocities to disk evolution in the terrestrial and Jovian planetary formation zones.

There are two other correlations between physical properties of the parent star and detectability of debris disks that have been reported in recent papers. Chen et al. (2005) obtained MIPS observations of a sample of about 40 F- and G-type members of the Sco-Cen association (age $\sim$5–20 Myr) and detected about one-third of them at 24 μm. They found an anticorrelation between disk excess and X-ray activity for their sample. They interpreted this in terms of the X-ray bright stars having strong winds, which could scour small dust particles from the debris disks in these systems. However, another correlation present in the Chen et al. (2005) data was that the stars with detected debris disks were preferentially earlier spectral types in their sample (hence higher mass if approximately the same age). A similar correlation between stellar mass and debris disk detection was noted by Wyatt et al. (2003) in a survey of the Lindroos (1986) sample of young nearby stars. The correlation between disk detection frequency and spectral type or mass may simply arise because smaller amounts of dust are more easily detected around more luminous stars, and therefore, the correlation between disk excess and X-ray activity found by Chen et al. (2005) may not require winds as the physical explanation. Determining whether there is a correlation between disk excess and X-ray activity for a sample of stars with a wide range of X-ray activity but a small range of mass would be a valuable step.

There have been several previous discussions of and/or searches for circumstellar dust around low-mass Pleiades members. Jones (1972) suggested that K dwarfs in the Pleiades were surrounded by dust shells in order to explain why those stars fell below the main sequence in a M_V versus $B-V$ color-magnitude diagram (CMD; for an alternative explanation of the CMD behavior not involving dust shells, see Stauffer et al. 2003). Backman et al. (1991) used the *IRAS* 25 and 60 μm data to search for IR excesses around a sample of Pleiades and IC 2391 A and early F dwarfs. They reported finding weak evidence for detecting an excess for the ensemble of IC 2391 stars but did not detect an excess for the Pleiades sample. Meyer & Beckwith (2000) used data from the *Infrared Space Observatory* (*ISO*) for another sample of A and F dwarfs in several nearby, young open clusters, including the Pleiades, but again were unable to detect IR excesses unambiguously in these stars. Spangler et al. (2001) also used the ISOPHOT instrument on *ISO* to search for debris disks around young stars. They observed 14 Pleiades low-mass members at 60 and 90 μm, with possible detections at one or both wavelengths for two of those members (HII 1132, an F dwarf, and HII 3163, a K dwarf). The *Midcourse Space Experiment* (*MSX*) was also used to observe the Pleiades (Kraemer et al. 2003), but it only detected the very brightest (B star) members of the cluster longward of 10 μm.

2. PROPERTIES OF THE PLEIADES STARS OBSERVED WITH *SPITZER*

All the main-sequence stars in the FEPS program were required to have $0.5 < B - V < 1.0$, and that criterion was applied to the Pleiades sample. Another significant constraint on our selection of Pleiades stars was that Legacy observations were required not to conflict with Guaranteed Time Observer (GTO) targets, and the N. Gorlova et al. (2005, in preparation) GTO program obtained a 1 deg^2 map of the center of the Pleiades using both IRAC and MIPS. Our FEPS targets are therefore located somewhat on the outskirts of the cluster. We also attempted to minimize difficulties caused by the extended IR emission from the gas and dust associated with the CO cloud impacting the Pleiades (White 2003) by avoiding stars within the region of high extinction identified by Breger (1987). Finally, some preference in selecting FEPS targets was given to stars not known to be binary. With these constraints in mind, the set of Pleiades members selected for *Spitzer* observation is provided in Table 1. All these stars are very high probability members of the cluster based on extensive radial velocity and proper-motion studies and on other indirect measures such as chromospheric and coronal activity and lithium abundance (Stauffer & Hartmann 1987; Soderblom et al. 1993).

The sources of the data in Table 1 are described in detail in J. Carpenter et al. (2005, in preparation); however, we provide a brief synopsis here. The V and $B-V$ data are generally derived from averaging the observations reported in Johnson & Mitchell (1958), Mendoza (1967), Stauffer (1984), and Stauffer &

TABLE 1
PLEIADES G AND K DWARF FEPS TARGETS

Name	V	$B-V$	$v \sin i$[a] (km s^{-1})	P (hr)	Binarity?	$\log (L_X/L_{bol})$
HII 120	10.81	0.70	9.4	...	SB1?	...
HII 152	10.73	0.69	11.4	...	N	...
HII 173	10.87	0.84	7.8/6.3	...	SB2	−4.20
HII 174	11.62	0.85	90:[b]	...	N	−3.05
HII 250	10.70	0.68	6.4	<24?	N	−4.06
HII 314	10.61	0.65	41.9	35.4	N	−3.22
HII 514	10.72	0.70	10.5	...	N	−4.22
HII 1015	10.54	0.65	9.6	...	N	−4.18
HII 1101	10.26	0.61	19.0	...	N	−4.24
HII 1182	10.46	0.64	16.4	...	VB	...
HII 1200	9.92	0.54	13.7	...	N	<−4.96
HII 1776	10.91	0.72	10.1	...	N	...
HII 2147	10.86	0.81	6.9/10.8	...	SB2	−2.94
HII 2278	10.90	0.87	6.9	...	VB	−3.82
HII 2506	10.25	0.60	13.8	...	N	...
HII 2644	11.07	0.75	4.3	...	N	−4.27
HII 2786	10.30	0.60	22.0	53.0	N	−4.30
HII 2881	11.54	0.96	10.5	102.0	VB	−3.30
HII 3097	10.94	0.74	14.6	...	SB1	...
HII 3179	10.05	0.56	4.9	...	N	−4.42

[a] For SB2s, $v \sin i$ values for both components are given.
[b] The colon indicates that this is a relatively uncertain measurement.

Hartmann (1987). The spectroscopic rotational velocities are from Queloz et al. (1998), except for HII 174 (from R. White et al. 2005, in preparation) and HII 1101 (from an average of values in Stauffer & Hartmann 1987; J.-C. Mermilliod 1993, private communication). Rotation periods have been reported for HII 250 (Messina 2001; Marilli et al. 1997), HII 314 (Prosser et al. 1993), HII 2786 (Krishnamurthi et al. 1998), and HII 2881 (Prosser et al. 1993). The rotation period for HII 250 may be spurious given the very small $v \sin i$ for this star; the star would have to be nearly pole-on if both the $v \sin i$ and rotation period are correct, but in that case one would expect very little photometric rotational modulation. Finally, the following stars in our list have been identified as binaries: HII 120 (Raboud & Mermilliod 1998); HII 173 (Stauffer et al. 1984; Mermilliod et al. 1992); HII 1182, HII 2278, and HII 2881 (Bouvier et al. 1997); HII 2147 (Queloz et al. 1998); and HII 3097 (Mermilliod et al. 1992). HII 1101 was also reported as being a spectroscopic binary (SB) in Soderblom et al. (1993) and Mermilliod et al. (1992). However, we believe that identification was spurious; careful examination of a number of spectra of this star does not support the SB designation. The X-ray data [$\log (L_X/L_{bol})$] in Table 1 are from Stauffer et al. (1994) and Micela et al. (1999).

Compared to the rest of the FEPS sample, the Pleiades sample might appear to include a higher fraction of binaries. However, that is at least in part illusory, owing to the fact that the Pleiades have been searched for binary stars more thoroughly than most of the FEPS targets. For example, Mermilliod et al. (1992) and Raboud & Mermilliod (1998) obtained more than 10 yr of accurate radial velocity monitoring of most of the Pleiades F, G, and early K dwarfs, allowing very good detection of short- and intermediate-period systems. Bouvier et al. (1997) obtained *JHK* adaptive optics (AO) imaging with the Canada-France-Hawaii Telescope (CFHT) in 1996 of most of the same stars, allowing detection of long-period binary companions with separations of 0.″1–6.″9 and *K*-band flux ratios up to 100. Metchev & Hillenbrand (2004) obtained *K*-band AO imaging of the Pleiades FEPS sample in 2002, allowing determination of common proper motion for possible companions detected in both surveys. Three of the Pleiades binaries would probably not have been identified as such if data similar to what is available for the average FEPS field dwarf were utilized. For example, HII 3097, an SB1 with period $P = 774$ days, eccentricity $e = 0.78$, and radial velocity amplitude $K1 = 5.1$ km s^{-1} (Mermilliod et al. 1992), has radial velocities that remain within about 2 km s^{-1} over about 80% of its orbital phase due to the high eccentricity of its orbit. Similarly, HII 120 is listed as a possible SB1 by Raboud & Mermilliod (1998) but with only a 3 km s^{-1} range in radial velocity over a 13 yr time span; this star would also have been unlikely to have been flagged as a binary in the rest of the FEPS sample. The companion to HII 1182 (Bouvier et al. 1997) was also detected in the FEPS team AO imaging program, but with $\Delta K \sim 4.8$ mag and a separation of 1.″14, we could have only listed it as a possible companion pending determination of common proper motion. Therefore, of the seven probable binaries in the Pleiades sample, only four would likely have been identified as such if they had been in our field star sample. The characteristics of the four "easily detected" binary systems in our Pleiades sample are:

HII 173: SB2, $P = 497$ days, $q \simeq 0.95$ (Mermilliod et al. 1992).

HII 2147: SB2, $P > 15$ yr, $q \sim 0.82$ (Queloz et al. 1998; Mermilliod et al. 1992).

HII 2278: VB, $\Delta K = 0.05$, separation 0.″37 (Bouvier et al. 1997), $q \sim 1.00$ (Mermilliod et al. 1992).

HII 2881: VB, $\Delta K \sim 0$, separation 0.″08 (Bouvier et al. 1997), $q \sim 0.81$ (Mermilliod et al. 1992).

Because the Pleiades stars are members of a cluster, they have a very well determined age, distance, and reddening, and hence a CMD can quite accurately identify binaries if the two stars have similar masses. We illustrate the latter point here as our Figure 1. The FEPS stars are indicated by circled dots, and the solid line is

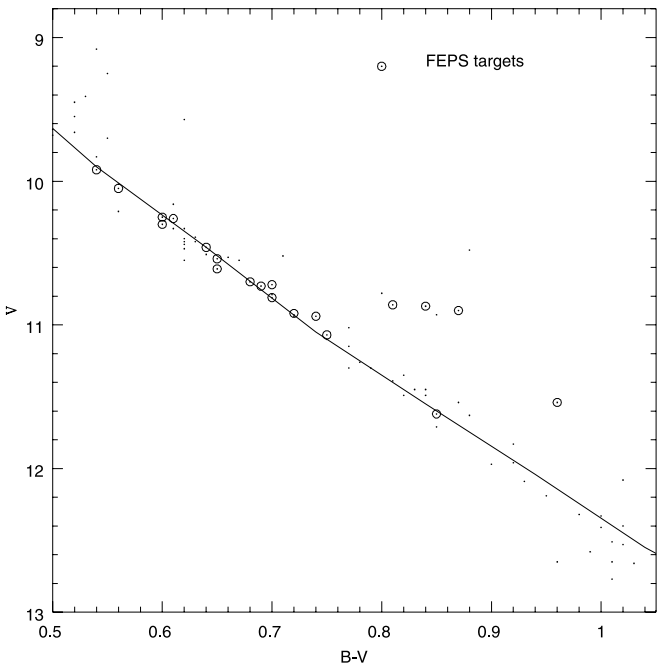

FIG. 1.—The V vs. $B - V$ color-magnitude diagram for Pleiades members derived from photoelectric photometry tabulated in J. Carpenter et al. (2005, in preparation). The FEPS targets are marked as circled dots, and the solid line is an empirical ZAMS.

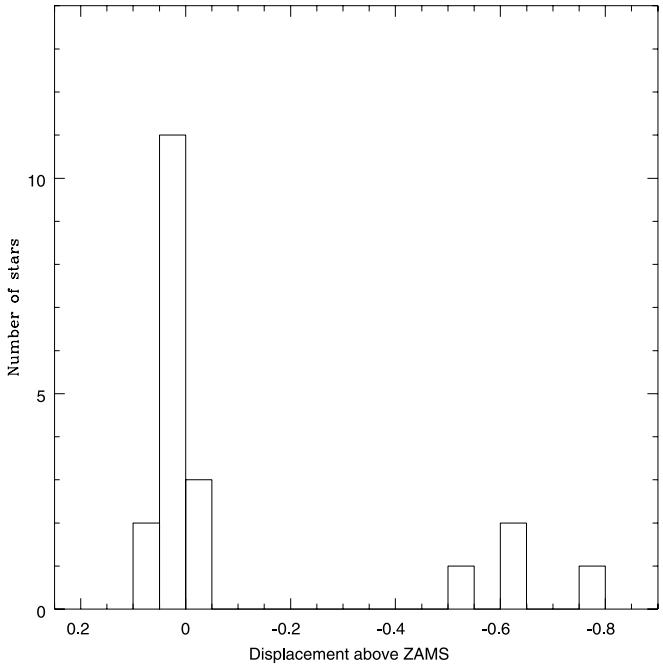

FIG. 2.—Displacement above the ZAMS curve of Fig. 1 for the Pleiades FEPS sample. The four stars to the right of the diagram are all known binaries with inferred secondary to primary mass ratios near 1.

simply an empirical ZAMS (drawn to follow the single-star main sequence defined by all Pleiades members; Johnson & Iriarte 1958). The "easily detected" binary systems are simple to identify in the plot: they are the four FEPS stars displaced above the main-sequence curve by more than 0.5 mag. Their displacement in the CMD is as expected from the fact that they are either SB2s or visual binaries with nearly equal magnitude components. Figure 2 provides a histogram of the displacements of the Pleiades FEPS stars relative to the ZAMS curve and indicates that, with the exception of the four $q \sim 1$ binaries, the FEPS Pleiades stars all lie within 0.1 mag of the single-star locus. Based solely on the CMD, therefore, one can conclude that these 16 stars do not have companions within about half the mass of the primary (at any separation) or, correspondingly, do not have companions within about 4 mag as bright as the primary (Mermilliod et al. 1992).

3. *SPITZER* OBSERVATIONS

The IRAC data for 19 of the 20 Pleiades FEPS targets were obtained during a single IRAC campaign in early September of 2004 (the one exception is HII 1776, for which IRAC observations had not been obtained at the time of the writing of this paper). All the IRAC observations were obtained in subarray mode, with data being obtained in channels 1, 2, and 4 (with central wavelengths of 3.6, 4.5, and 8.0 μm, respectively). The integration time per exposure was set to 0.08 s for the three brightest stars and to 0.32 s for the remainder. Each target was observed at four dither positions. In subarray mode, 64 exposures are obtained at each position, and therefore 256 exposures were obtained for each star. The pipeline processing software used at the *Spitzer* Science Center (SSC) for the data we analyzed was S10.5.[3] We used the analysis package IDP3 (Schneider & Stobie 2002) to derive aperture photometry from the basic calibrated data (BCD) images provided to us by the SSC. An aperture size of 3 pixels was used, with multiplicative aperture corrections of 1.112, 1.113, and 1.218, respectively, for channels 1, 2, and 4. See Silverstone et al. (2005) for more details concerning the method used to analyze the IRAC BCD images.

IRS spectra for all 20 Pleiades FEPS targets were obtained during 2004 September 26 and 27. The spectra cover the wavelength range from 7.4 to 38 μm at relatively low resolution ($\lambda/\Delta\lambda \simeq 70-120$). We began each observation (each "AOR") with a high-accuracy peak-up using the short-wavelength side of the IRS peak-up array in order to ensure that the Pleiades star was accurately centered in the spectrograph slits. This worked well except in one case: for HII 2881, another object (presumably an IR-bright, distant galaxy) was brighter than HII 2881 in the peak-up array bandpass, and the spectra we obtained were therefore of the galaxy. For this reason, we do not have IRS spectra of HII 2881. The total integration times for our targets depended on the predicted mid-IR flux, with a minimum of about 90 s in the short-low module and 500 s in the long-low modules to a maximum of about 240 s in the short-low module and 2770 s in the long-low modules. As the starting point for our analysis, we used the two-dimensional "droop" spectral images, i.e., the intermediate data product produced by the S11.0.2 pipeline, prior to flat-fielding or stray-light correction. To extract the spectra, we use the SMART software package (S. Higdon et al. 2005, in preparation). The spectra were extracted using a fixed-width aperture of 6.2 pixels for the first order of the short-wavelength low-resolution module and 5.1 and 3.1 pixels for the first and second order of the long-wavelength low-resolution module, respectively. We corrected for the sky background and possible stray light by subtracting the two nod positions observed along the slit. The spectra were calibrated using a spectral response function derived from a set of IRS spectra and stellar models of 16 stars observed within the FEPS program (see J. Bouwman et al. [2005, in preparation] and the

[3] The IRAC channel 1 flux calibration in the S10.5 pipeline had a slight systematic error (which was corrected in S11). We have adjusted our derived in-band fluxes for channel 1 downward by 7% to correct for this, consistent with the improved S11 flux calibration.

TABLE 2
Spitzer Data for the Pleiades FEPS Targets

Name	*K* (mag)	IRAC 3.6 μm (mag)	IRAC 4.5 μm (mag)	IRAC 8.0 μm (mag)	MIPS 24 μm (mag)	IRS 24 μm (mJy)	IRS 33 μm (mJy)	MIPS70 μm[a] (mJy)
HII 120.....	9.103	9.075	9.113	9.119	9.06	1.41	0.48	<36
HII 152.....	9.12	9.069	9.108	9.119	8.98	2.19	2.09	<27
HII 173.....	8.827	8.797	8.852	8.844	8.83	2.03	1.24	<23
HII 174.....	9.374	9.292	9.344	9.330	9.33	0.66	−0.07	<17
HII 250.....	9.061	9.043	9.061	9.074	8.94	2.01	1.71	<15
HII 314.....	8.900	8.876	8.921	8.918	8.89	2.03	1.74	<23
HII 514.....	9.041	9.026	9.064	9.060	8.86	2.33	2.00	<15
HII 1015.....	8.993	8.958	8.985	8.997	9.01	0.56	−0.05	<30
HII 1101.....	8.76	8.735	8.766	8.775	8.34	3.92	4.07	<24
HII 1182.....	8.928	8.917	8.955	8.963	8.92	1.85	1.10	<10
HII 1200.....	8.546	8.512	8.533	8.572	8.41	3.15	2.27	<43
HII 2147.....	8.60	8.555	8.596	8.605	8.59	3.05	1.50	<10
HII 2278.....	8.805	8.739	8.791	8.775	8.78	1.70	0.72	<23
HII 2506.....	8.796	8.805	8.844	8.862	8.85	1.93	1.25	<15
HII 2644.....	9.307	9.302	9.350	9.358	9.34	1.36	0.14	<15
HII 2786.....	8.853	8.832	8.858	8.880	8.88	1.90	0.92	<16
HII 2881.....	9.054	9.060	9.087	9.082	9.07	...	...	<12
HII 3097.....	9.137	9.070	9.113	9.119	9.09	1.60	0.62	<10
HII 3179.....	8.632	8.623	8.657	8.694	8.68	2.42	1.21	<10

Notes.—IRAC flux zero points: 277.5, 179.5, and 63.1 Jy for 0 mag for channels 1, 2, and 4, respectively (Fazio et al. 2004); the fluxes are not color-corrected. The 1 σ statistical random uncertainties for all three IRAC bands are ~2%. MIPS flux zero point: 7.20 Jy for 0 mag for MIPS24 (from the MIPS Data Handbook, ver. 2.3, and from data for FEPS G dwarfs older than 1 Gyr for which no excess is expected). Typical 1 σ statistical random uncertainties for the MIPS24 fluxes are 50 μJy.

[a] The indicated values are 3 σ upper limits; none of the stars are clear detections at MIPS70. The average 1 σ noise for these measurements is about 7 mJy, but some of the stars have visible cirrus or faint objects near them, and their noise level is higher.

explanatory supplement to the FEPS data at the SSC data archive for further details on IRS data reduction). For the purpose of using the spectra to test quantitatively for IR excesses above the photospheric flux, we have defined pseudobandpasses at 24 and 33 μm, assuming a filter response function for the IRS24 band identical to that for MIPS24 and a square bandpass running from 30 to 35 μm for IRS33. We integrated the spectra over these bandpasses to derive in-band fluxes, which we designate as IRS24 and IRS33.

The MIPS data for 19 of the 20 Pleiades FEPS targets were obtained during a single MIPS campaign; more specifically, the Pleiades stars were observed in an 8 hr window on 2004 September 22 (with all 19 targets being observed consecutively). The one star lacking MIPS data is again HII 1776. The MIPS small-field photometry mode was used. At 24 μm, four cycles of 10 s exposures were obtained for all the targets, corresponding to a total of about 600 s of integration time per source. At 70 μm, the on-source time was varied depending on the brightness of the star and the expected background, with a range from about 230 s to about 1090 s. For 24 μm, we based our analysis on BCD and post-BCD data from the S10.5 pipeline processing by the SSC. Because the Pleiades stars are relatively faint and the background (Pleiades nebular structures, field stars, and background active galactic nuclei [AGNs]) is complex, we deviated from the standard FEPS analysis of the MIPS 24 μm data. In particular, instead of aperture photometry, we derived point-spread function (PSF)–fitting photometry using the APEX software package (D. Makovoz et al. 2005, in preparation) with a 24 μm PSF constructed from a MIPS map obtained as part of the *Spitzer* First Look Survey. To maximize the signal-to-noise ratio of the measurement, only the central 2 pixel radius of the PSF was used to scale the PSF and to derive our flux estimates. For MIPS 70 μm, we used the raw data together with the MIPS team's DAT software package (Gordon et al. 2005) to produce final, mosaicked images (see Kim et al. [2005] for details). We do not detect any of our targets with confidence at 70 μm. We therefore followed the standard FEPS practice of deriving upper limits (or measured fluxes) from the MIPS 70 μm images using aperture photometry, with a 3 pixel radius aperture.

The *Spitzer* data for the Pleiades FEPS targets are provided in Table 2. The data for IRAC and MIPS24 are given in magnitudes; the data for IRS24, IRS33, and MIPS70 are given in mJy. For pure photospheres, G dwarfs are expected to have essentially constant magnitude at *Spitzer* wavelengths; hence, by presenting the data in magnitudes, one can very quickly scan the table and ascertain that most of the Pleiades stars have no significant IR excess through 24 μm. The IRS and MIPS70 data are given in mJy because there is no zero-point calibration available to define a magnitude system for IRS and because some of the IRS and MIPS in-band fluxes are negative (consistent with nondetection within the errors) and hence cannot be straightforwardly represented as magnitudes. Flux zero points for the IRAC and MIPS24 bandpasses are provided at the bottom of the table. Based on a combination of the internal uncertainty estimates provided by our software routines, the consistency checks we have made (some of which are described below), and other tests we have made using data for the older stars in the FEPS sample, we believe that the typical 1 σ statistical random uncertainties in our flux estimates are 2% for IRAC, 50 μJy for MIPS24 (i.e., also about 2%), 0.4 mJy for IRS24, 0.45 mJy for IRS33, and about 7 mJy for MIPS70. Note, however, that these estimated 1 σ uncertainties are specific to the manner in which the observations were obtained; for each instrument, our observations were obtained in a very homogenous fashion and during a single campaign (for MIPS, during a single, uninterrupted 10 hr period). This likely results in relative uncertainties that are smaller than is typically true for random data sets.

As the simplest means to assess whether any of the Pleiades FEPS targets shows evidence of an excess in the mid-IR, Figure 3 shows the distribution of the *K* minus MIPS24 magnitude

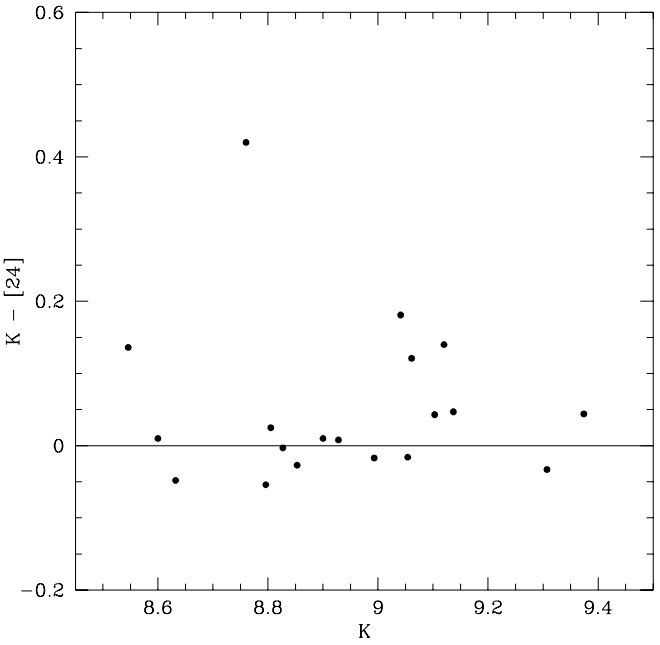

FIG. 3.—Difference between the *K*-band magnitude and the MIPS 24 μm magnitude for the Pleiades FEPS stars as a function of *K*-band magnitude. For solar-type stars, the difference should be approximately zero for a pure photosphere. The five stars with $K-[24]$ magnitude differences greater than 0.1 are stars with possible excesses due to circumstellar debris disks. The horizontal line simply marks equality between the two magnitudes. The stars with the largest $K-[24]$ colors are HII 1101 ($K-[24]=0.420$) and HII 514 ($K-[24]=0.18$).

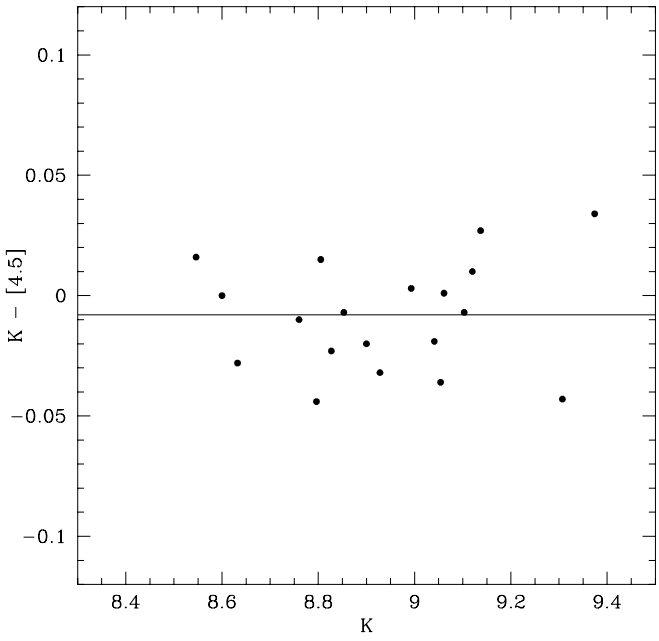

FIG. 4.—Difference between the *K*-band magnitude and the 4.5 μm magnitude for the Pleiades FEPS stars as a function of *K*-band magnitude. For solar-type stars, the difference should be approximately zero for a pure photosphere. Because the Pleiades stars are all likely low-amplitude photometric variables, the dispersion about zero represents an upper limit to the relative photometric accuracies of the *K* and IRAC channel 2 data. The horizontal line indicates the mean $K-[4.5]$ color for the Pleiades stars.

difference for our sample. The fact that most of the stars are distributed within 5% of $\Delta\mathrm{mag}=0.00$ in this diagram indicates that (1) most of the Pleiades stars do not have excesses and (2) the use of the 2.2 μm flux plus a Rayleigh-Jeans approximation to predict the photospheric flux at 24 μm works quite well. The five stars with apparent excesses exceeding 0.1 mag are potential debris disk detections, which we examine in more detail in § 4.

4. INITIAL ANALYSIS: DO THE PLEIADES G DWARFS HAVE DETECTED DEBRIS DISKS?

Because the *Spitzer* data cover a broad wavelength regime, we are able to detect dust with a wide range in temperature. The excesses that we expect might be present are small, however, and an important facet of our analysis is an investigation to verify that any excesses we detect are real. If the Pleiades stars do indeed have mid-IR excesses, we need to determine how well our measurements constrain parameters describing the circumstellar dust around these stars and hence our ability to provide quantitative constraints on debris disk evolution for stars of mass similar to the Sun's. We address these questions in §§ 4.1 and 4.2.

4.1. *Do the Pleiades G Dwarfs Have Excesses at IRAC Wavelengths?*

Based on standard, prelaunch model predictions, we did not expect our 100 Myr old Pleiades G dwarfs to have a sufficient amount of warm ($T>300$ K) circumstellar dust to yield detectable excesses at IRAC wavelengths. Nevertheless, we believe it is worthwhile to check our IRAC data carefully for this possibility. First, IRAC provides the most sensitive and potentially the most stable camera at these wavelengths to date, and hence it may be possible to detect excesses from zodiacal-like dust that would have escaped previous surveys. Second, a few of the Pleiades A dwarfs show excesses at 8 μm and at longer wavelengths (J. Stauffer et al. 2005, in preparation; N. Gorlova et al. 2005, in preparation). We believe that at least in most cases those excesses are not due to circumstellar dust disks but are instead the product of interstellar dust (mostly emission from polycyclic aromatic hydrocarbons) from the colliding molecular cloud being lit up by close passage by the Pleiades stars. Detection of an 8 μm excess in any of our Pleiades G dwarfs might be a signature of this phenomenon rather than of a debris disk and complicate the interpretation of any excess we detect at longer wavelengths.

In practice, we do not see any evidence for excesses at IRAC wavelengths. Figure 4 illustrates this via a plot of the $K-[4.5]$ color for our Pleiades stars, while Figure 5 shows the $[4.5]-[8.0]$ color for our targets. We expect these colors to be essentially zero for G dwarfs, and to within 0.01 mag the mean colors are zero for our sample (the mean color is -0.008 in both cases). The absolute calibration of the IRAC photometry is not sufficiently well known to consider these mean offsets as real. The dispersion about the $K-[4.5]$ mean color is 0.023 mag, which is barely larger than the expected 0.02 mag uncertainty for the Two Micron All Sky Survey (2MASS) *K* magnitudes. The dispersion about the $[4.5]-[8.0]$ mean color is only 0.014 mag, indicative of both a lack of warm dust in the Pleiades G dwarfs and the very good differential photometry possible with IRAC.

4.2. *Do the Pleiades G Dwarfs Have Excesses at $\lambda > 10$ μm?*

In Figure 3, we used the $K-24$ μm color as a simple means to identify stars with mid-IR excesses. A potentially more sensitive test can be made by fitting a Kurucz model photosphere to the existing optical and near-IR photometry for each star and then subtracting that photosphere from the *Spitzer* photometry. Table 3 provides our predicted model in-band fluxes for MIPS24, IRS33, and MIPS70. The IRS24 model fluxes are identical to those for MIPS24. The formal 1 σ uncertainties for each of the predicted model in-band fluxes ranges from about 2.5% to 5%, with typical values of order 4%.

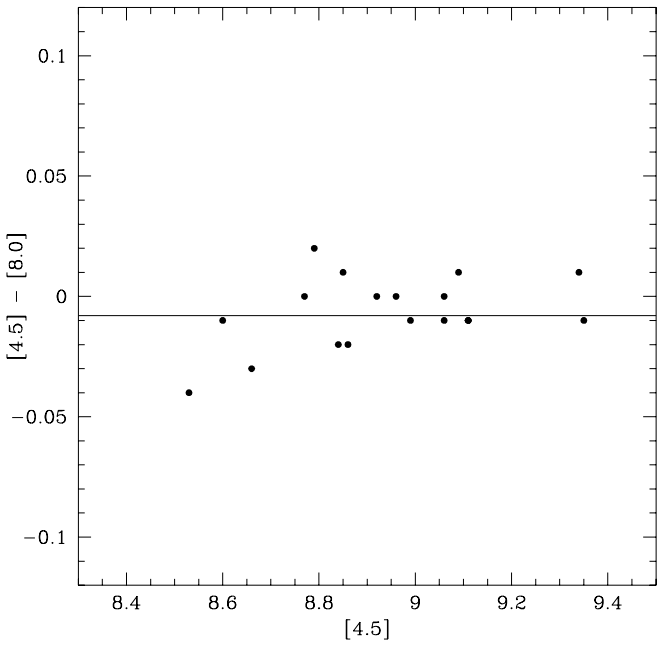

FIG. 5.—Difference between the channel 2 (4.5 μm) magnitude and the channel 4 (8.0 μm) magnitude for the Pleiades FEPS stars. For solar-type stars, the difference should be approximately zero for a pure photosphere. These observations are obtained simultaneously, so they are unaffected by the likely intrinsic variability of the Pleiades stars. The horizontal line indicates the mean [4.5]−[8.0] color for the Pleiades stars.

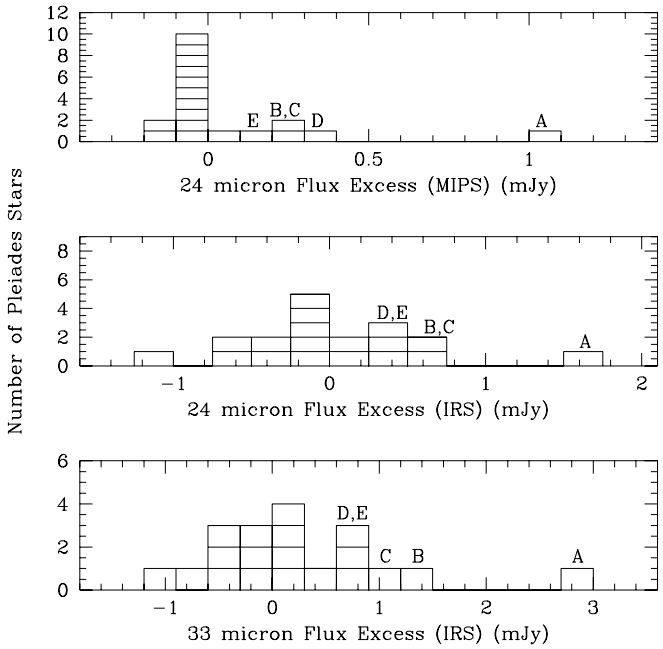

FIG. 6.—Differences between our measured in-band fluxes for MIPS24, IRS24, and IRS33 and predictions from best-fit Kurucz models that have been scaled to the published optical and near-IR photometry for our targets. The labeled histogram boxes mark the positions of HII 1101 (*A*), HII 152 (*B*), HII 514 (*C*), HII 1200 (*D*), and HII 250 (*E*). See the text for a discussion.

Figure 6 shows histograms of the flux excesses (observed flux minus photospheric estimate) for MIPS24, IRS24, and IRS33. Each histogram is characterized by a set of stars whose calculated excesses scatter about zero and a small set of stars populating a tail to positive excess, representing possible debris disk detections. Is this tail of IR-bright stars simply ascribable to random errors, or is it indicative of a population of stars with real excesses? Evidence for the latter conclusion is provided by marking the location of five particular stars in the three histograms: HII 1101 (*A*), HII 152 (*B*), HII 514 (*C*), HII 1200 (*D*), and HII 250 (*E*). With only one exception, these five stars are the highest excess objects in each histogram, usually in the same order. They are also the same five stars with $K-$MIPS24 colors greater than 0.1 mag highlighted in Figure 3. For MIPS24, all five have excesses at 4 σ or greater above the photospheric prediction. We conclude that there is real excess flux in our aperture toward these stars. However, the excess flux is not necessarily associated with our Pleiades stars.

TABLE 3
PREDICTED PHOTOSPHERIC FLUXES FOR FEPS TARGETS

Name	MIPS 24 μm (mJy)	IRS 33 μm (mJy)	MIPS 70 μm (mJy)
HII 120.....	1.677	0.887	0.188
HII 152.....	1.619	0.854	0.181
HII 174.....	1.299	0.687	0.146
HII 173.....	2.196	1.163	0.246
HII 250.....	1.704	0.900	0.191
HII 314.....	2.010	1.065	0.226
HII 514.....	1.793	0.949	0.201
HII 1015.....	1.846	0.975	0.206
HII 1101.....	2.231	1.177	0.249
HII 1182.....	1.939	1.024	0.217
HII 1200.....	2.785	1.473	0.311
HII 1776.....	1.591	0.842	0.178
HII 2147.....	2.669	1.416	0.300
HII 2278.....	2.286	1.213	0.257
HII 2506.....	2.228	1.178	0.249
HII 2644.....	1.385	0.732	0.155
HII 2786.....	2.097	1.108	0.234
HII 2881.....	1.755	0.929	0.197
HII 3097.....	1.679	0.889	0.188
HII 3179.....	2.559	1.353	0.286

The long-wavelength excesses could, in principle, be due to chance alignments of our targets with uncataloged asteroids. However, because the IRS and MIPS data were obtained at significantly different dates yet the same stars show up with possible excesses, we believe that asteroids are not likely to be the cause of the excesses. Instead, the most likely contaminant to the 24 μm in-band fluxes is confusion from random line-of-sight positional overlap with (1) distant, optically faint but IR-bright AGNs or (2) inhomogeneities (cloudlets? filaments?) in the Pleiades nebular emission. One way to determine whether contamination is a problem is to look for positional offsets between the measured MIPS24 positions of our targets and the input positions for each AOR (which come from 2MASS for our targets). This test is only possible because of the excellent pointing accuracy and stability of *Spitzer*; IRAC observations indicate that the "blind-offset" positional accuracy for *Spitzer* is generally about 0.″25, with an rms of similar magnitude. Figure 7 shows the positional offset between the 2MASS and MIPS24 centroids for the Pleiades stars, with the five potential excess sources highlighted. One excess star, HII 152, is clearly an outlier. If we exclude that star, the mean positional offsets are ΔR.A. $= 0.''62$ and Δdecl. $= -0.''24$; the rms of the radial positional error is 0.″27, in excellent agreement with the expected pointing accuracy of *Spitzer* and suggestive that other sources of error (e.g., AGN contamination) do not significantly affect the Pleiades measurements in general. Of the possible excess sources, HII 152 has a >3 σ offset from its expected position, suggesting that its 24 μm flux is probably

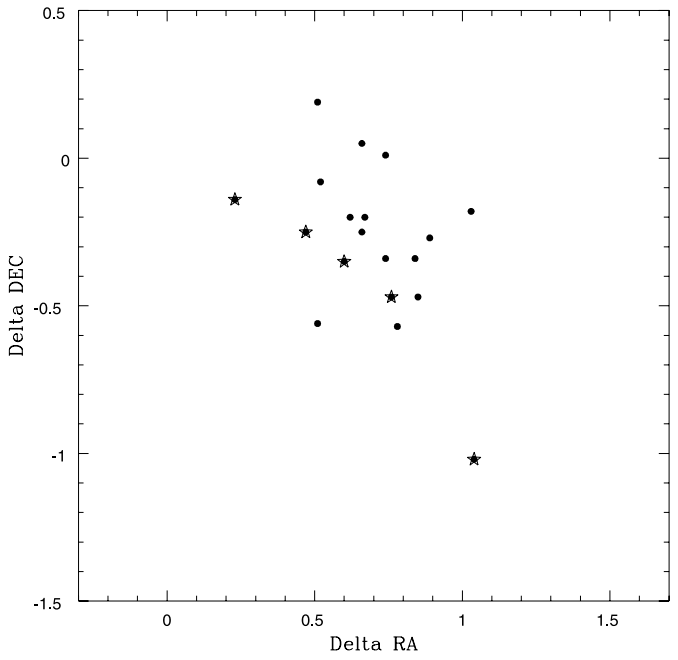

FIG. 7.—Offset (in arcseconds) between the 2MASS position of the Pleiades FEPS stars and the measured centroid positions from the MIPS24 images. The star symbols mark the five stars with the largest 24 μm excesses (HII 152, 250, 514, 1101, and 1200); it is HII 152 that is at ΔR.A. $\sim 1''.0$, Δdecl. $\sim -1''.0$. The large positional offset relative to the mean for HII 152 is evidence that its 24 μm excess is probably due to contamination of our flux measurement by local cirrus or a background AGN near the line of sight.

contaminated. HII 250 is the next most discrepant point (at δdecl. $\sim -0''.13$, δR.A. $\sim 0''.23$). The other three stars from Figure 7 (HII 1101, 514, and 1200) have positional offsets relative to the mean of the distribution $<0''.3$, consistent with no contamination.

Another means to assess whether an additional object near the line of sight to our Pleiades stars is affecting our MIPS24 photometry is to do PSF subtractions. We have done that for our five stars with the largest possible 24 μm excesses. We performed two experiments: (1) subtract a 24 μm PSF scaled to the measured flux from the mosaicked 24 μm (post-BCD) image, and (2) subtract a 24 μm PSF scaled to the predicted flux from the Kurucz model. Only HII 152 showed any evidence for a distorted, inner PSF in these experiments. However, both HII 152 and HII 250 showed evidence of an extended, very low level pedestal of emission (above the average sky background) extending 5–10 pixels from the star. Because this is too large an angular extent to be indicative of a dusty debris disk centrally heated by our target star, we assume it is indicative of a local condensation of the interstellar nebulosity in the Pleiades, projected toward the line of sight. To help further elucidate the nature of the possible 24 μm excesses, we also determined aperture growth curves (for apertures from 2 to 7 pixel radius) for the five possible excess stars and for a sample of the stars with no apparent excess. Most of the stars—including HII 1101, the star with the largest excess—showed growth curves consistent with expectation for the STINYTIM model PSF. Both HII 152 and HII 250 show growth curves that are broader than that expected for pure point sources, consistent with extended local nebular emission in the source aperture above the background estimated from our 10–20 pixel radius sky annulus. For both these stars, the growth curves are well matched by a model consisting of a standard PSF plus a constant excess sky out to a 7 pixel radius. However, the predicted effect on our PSF-fitting flux of this local excess nebular emission is only about one-third of the excess that we measured (Table 2). Either the local nebular emission must have a sharp peak at the location of HII 152 and HII 250, or other effects may also be influencing their 24 μm flux. HII 514 and HII 1200 show slight irregularities in their growth curves due to a faint companion at 4.5 pixel distance for HII 514 and probably due to local cirrus for HII 1200. We believe the PSF flux we report for them is correct but with less certainty than for most of our stars.

Finally, it is possible to estimate the number of expected cases in which a background, IR-bright galaxy would affect our MIPS Pleiades photometry based on *Spitzer* 24 μm source-count statistics (Papovich et al. 2004). Figure 2 of that paper shows cumulative 24 μm source count data derived from several different high-latitude fields; that plot indicates expected cumulative source counts of order 10^6 sr^{-1} for objects with 24 μm flux >1 mJy and 10^7 sr^{-1} for objects with 24 μm flux >0.3 mJy. First, consider HII 1101, our star with the largest excess at 24 μm, about 1 mJy. The cumulative counts for that flux level correspond to about one source per 40,000 arcsec^2. In order for a 1 mJy source to displace the centroid position of HII 1101 by less than $0''.3$, it would have to be located less than $1''$ from HII 1101 (given HII 1101's photospheric flux at 24 μm of 2.2 mJy and assuming our measured excess is due to a background galaxy). The a posteriori probability of a background galaxy with 24 μm flux $\geq$1 mJy being this close to the line of sight to HII 1101 is therefore less than 1 in 10,000. For our sample of 20 targets, there is then an $\sim$1 in 500 chance that 1 of them would have had this happen, supporting our belief that the excess for HII 1101 has a high probability of being real. Would AGN contamination provide a plausible explanation for the large positional error and 24 μm excess we found for HII 152? Compared to HII 1101, the 24 μm excess for HII 152 is smaller, of order 0.3 mJy, and the derived 24 μm positional error is larger, of order $0''.9$. Using the 10^7 sources sr^{-1} number appropriate for this flux level, we derive a probability of a background source being this close to the line of sight of a given Pleiades star of order 1 in 40. Therefore, for our sample of 20, we should have expected a 50% probability that one of them would have had the properties we found for HII 152, supporting AGN contamination as a plausible explanation for the 24 μm excess of this star. With fairly similar properties, HII 250 is also a good candidate for AGN contamination. Lastly, we consider the other two possible excess sources, HII 514 and HII 1200 (MIPS24 flux excess of about 0.3 mJy, MIPS24 positional offset $<0''.3$, and photospheric flux of $\sim$2 mJy). We derive about a 1 in 400 chance of this alignment for a single target, or about a 5% probability that one of our sample of 20 would have such an alignment. We conclude that the excesses for HII 514 and HII 1200 are plausibly real but with significantly less confidence than for HII 1101. In summary, our best judgments for the five stars with 24 μm excesses are:

HII 152: Very likely contaminated by cirrus or a background AGN; not a debris disk.

HII 250: Probably contaminated by cirrus or a background AGN.

HII 514: Possible debris disk.

HII 1200: Possible debris disk.

HII 1101: Probable debris disk.

5. DISCUSSION

5.1. *Physical Interpretation of the Excesses and Upper Limits*

Figure 8 shows the spectral energy distributions (SEDs) for the Pleiades FEPS target with the best evidence for mid-IR excess (HII 1101) and one of the two stars with possible excesses

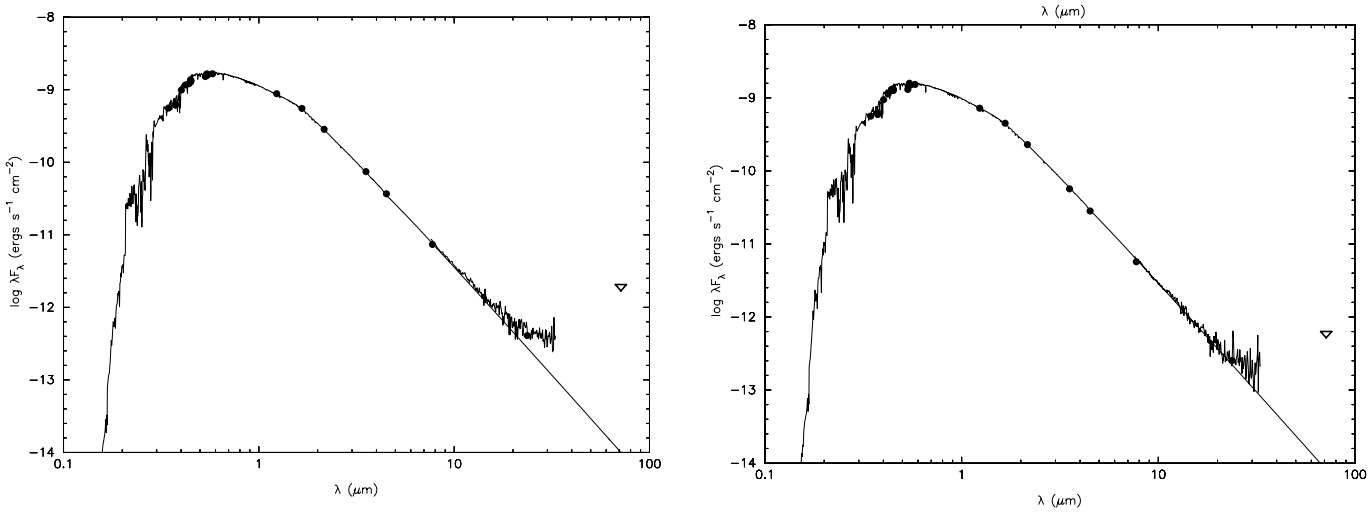

FIG. 8.—SEDs and best-fit Kurucz models for the two Pleiades stars with the best evidence for mid-IR excesses (*left*: HII 1101; *right*: HII 514).

(HII 514). The solid black line in the figure is a best-fit Kurucz model whose parameters were determined from a least-squares fit to the optical and near-IR photometry. We used published *BVRIJHK* photometry to normalize the Kurucz model spectra.

For the purposes of the physical model fits, we assume a Pleiades distance of 133 pc, which is the average of several recent determinations using astrometric observations of binary star Pleiades members (Pan et al. 2004; Zwahlen et al. 2004; Munari et al. 2004), direct trigonometric parallax using the *Hubble Space Telescope* (Soderblom et al. 2005), and metallicity-corrected main-sequence fitting (Percival et al. 2005). In order to convert our observables to something more physical that can be usefully compared, for example, to our solar system's Kuiper Belt or to debris disks of other ages, it is useful to calculate a few physical parameter constraints for our Pleiades sample based on a specific, simple model. We describe this model in detail below. This particular model provides minimum dust grain masses that are consistent with our *Spitzer* data.

We fit the excess SED (observations minus estimated photosphere) with a simple blackbody grain model based on the color temperatures (T_c) calculated from the Planck formula and the ratio of excess fluxes measured in the MIPS bandpasses and our IRS33 bandpass. Increasing excess-flux densities between $<$24 and 33 μm indicate that we are observing the Wien side of the SED, with the color temperature corresponding approximately to the maximum dust temperature in the disk and hence the minimum distance from the star of the emitting material. The relationship between grain temperature, position, and primary star luminosity (Backman & Paresce 1993) for blackbody grains that absorb and emit radiation efficiently at all observed wavelengths is

$$R_{\rm inner} = \left[(278\ {\rm K})(L_*/L_\odot)^{0.25}/T_c\right]^2. \quad (1)$$

The derived dust temperature T_c, observed excess-flux densities, and cluster distance can then be used with the Planck and Stefan-Boltzmann equations to calculate a total grain cross-sectional area and dust luminosity. An estimate for the total dust mass can then be derived from the cross-sectional area by assuming a material density and a characteristic grain radius consistent with the assumption of blackbody emission to the maximum wavelength of the observed excess (Kim et al. 2005). The total radiating dust mass estimates derived are minimum values, because (1) they are derived from the dust maximum temperature, whereas a broader radial range including lower temperature dust would have more mass for a given luminosity, and (2) they assume a single dust grain size, whereas dust with a size distribution (e.g., a standard MRN model [Mathis et al. 1977] in which $n \propto a^{-3.5}$, where a is the grain radius and n is the number density of grains of size less than or equal to a) has most of the luminosity arising from the smallest grains but most of the mass residing in the largest grains.

For HII 1101, following the process described above, the inferred 24 to 33 μm color temperature ratio of the excess is 84 K. Using this color temperature, we derive $R_{\rm inner} = 12.6$ AU. For our measured MIPS 24 μm excess of 1.09 mJy, we obtain a dust solid angle of 4.8×10^{-16} sr, and with 133 pc for the distance to the Pleiades we then derive the total dust cross-sectional area of $A = 0.34$ AU^2. With a generic silicate density of 2.5 g cm^{-3} and a dust radius of 10 μm, this yields a lower limit to the dust mass of $\log(M_{\rm dust}/M_\bullet) = -4.4$ and a fractional dust luminosity of $\log(L_{\rm dust}/L_*) = -3.8$.

We can place an upper limit to the debris disk mass for the $\sim$17 Pleiades solar-mass stars for which we do not detect mid-IR excesses. Using the same formalism as for HII 1101, the grain temperature derived for HII 1101, and the 3 σ rms upper limits for the nondetected stars, 150 μJy and 21 mJy, respectively, for MIPS24 and MIPS70, we derive estimated 3 σ upper limits for a dust mass of $\log(M_{\rm dust}/M_\bullet) = -5.2$ and -3.8. Because the fluxes radiated at the shorter wavelengths are more dependent on the details of the dust grain size distribution and composition and the radial distribution of dust, the dust mass upper limit for MIPS70 is less model dependent than that for MIPS24.

The SED for HII 1101 implies that there is less dust radiating at temperatures above 84 K than at or below 84 K. A rough estimate of an upper limit to the amount of material with $T > 84$ K ($r < R_{\rm inner} \sim 12.6$ AU, where r is the distance from the star) can be calculated such that emission from the warm dust would not exceed 1 σ above the observed SED already fit by the photospheric emission plus blackbody dust excess model described above. We assume a distribution of dust extending from 12.6 AU to silicate sublimation at $T \sim 1500$ K ($r \sim 0.04$ AU) with a radially constant surface density consistent with dynamics controlled by Poynting-Robertson (PR) drag. Under these assumptions the upper limit on dust warmer than

84 K is $\log (M_{\rm dust}/M_{\bullet}) < -5.7$. There is evidently a central zone relatively depleted of dust inside the zone in which dust is detected. The blackbody grain model described above would require something to prevent the dust grains generated in a planetesimal belt beyond 13 AU from spiraling into the inner dust due to PR drag. While other models cannot be ruled out, it is interesting to note that the presence of a giant planet inside 13 AU could be responsible for the inner hole (Kim et al. 2005).

5.2. *Implications for Debris Disk Evolutionary Timescales*

How do our observed properties of solar-mass stars in the Pleiades compare to what we believe the debris disk for an average star like the Sun should look like at an age of 100 Myr? We address this question by using a simplified evolutionary model of our solar system's Kuiper Belt (Kim et al. 2005; D. Backman et al. 2005, in preparation). The model combines collisional evolution of the Kuiper Belt planetesimal population with quasi-equilibrium dust production and dust spatial redistribution (Backman et al. 1995). A parallel model of the evolution of the asteroid belt and its associated zodiacal dust cloud predicts negligible far-IR contribution from the inner solar system relative to the outer solar system at the ages of the Pleiades stars.

The model includes the effects of much stronger winds predicted from young low-mass stars. In particular, at the Pleiades age we assume a wind mass-loss rate 1000 times the current solar wind, following Wood et al. (2002). The effect of this wind is to add an additional scouring mechanism acting preferentially to remove small grains, hence primarily affecting emission at shorter wavelengths. For the Pleiades age, a model with 1000 times solar wind mass-loss rate shows a 60% decrease in the 24 μm flux density but only a 25% decrease in the predicted 70 μm flux density relative to a model with wind like the present-day Sun's.

In order to be generic, the model does not include some effects that could significantly affect the debris disk characteristics at the Pleiades age but that are dependent on dynamical evolutionary events that are neither deterministic nor easily incorporated into a simple model like ours. In particular, our model implicitly assumes that the orbits of the major planets did not change significantly between the Pleiades age and the present. Some current research indicates that considerable orbital migration may have occurred in our solar system after an age of 100 Myr (Levison et al. 2004; Morbidelli et al. 2005), including events that could have temporarily greatly enhanced or reduced the IR luminosity of our system. Our model also does not account for individual rare large planetesimal collisions temporarily injecting large amounts of dust, which would have been more common in earlier eras.

With the above caveats, the predicted flux densities for 133 pc, 100 Myr, and a solar-mass star (and hence for a luminosity 80% that of the present-day Sun's) are 0.4 mJy at 24 μm and 12 mJy at 70 μm. Those numbers bracket our 3 σ upper limits for the nondetected Pleiades G dwarfs at those two wavelengths. Each individual Pleiades star is therefore roughly consistent with the prediction of the heuristic model. However, as an ensemble, the mean observed 24 and 70 μm excess fluxes for the Pleiades G dwarfs are below the predictions of the model. We note that if one simply put the Sun and *present-day* solar system dust at Pleiades distance, the approximate 24 and 70 μm flux dust excesses we would observe would be of order a few μJy at 24 μm and of order 50 μJy at 70 μm, well below what is detectable with *Spitzer*.

5.3. *Correlations with Other Stellar Properties*

With only one to possibly three stars with detected excesses, our statistical base is too small to draw any definitive conclusions concerning the correlation between IR excess and other stellar properties. Hence, we cannot yet address with any certainty the questions raised in § 1 concerning possible correlations between debris disks and stellar mass, rotation, and X-ray luminosity. In any event, our probable excess star (HII 1101) and our two possible excess stars (HII 514 and HII 1200) are fairly unremarkable in most of their properties. They are not known to be binaries, but that is also true of most of our targets. Their projected rotational velocities are average for our FEPS Pleiades sample (see Table 1) and average for stars of their age. Only three of our Pleiades stars have rotational velocities more than 20 km s^{-1}; those three stars do not have excesses, but >80% of our stars do not have excesses. HII 1200 is the most massive star in our sample, HII 1101 is the fourth or fifth most massive star, while HII 514 is average in terms of its inferred mass. This is perhaps slight evidence in favor of the trend noted in § 1 in other data sets for the stars with detected debris disks to be higher mass. There is a weak correlation in our data between X-ray activity [$\log (L_{\rm X}/L_{\rm bol})$ in Table 1] and debris disk detection in the same sense as seen by Chen et al. (2005), since our Pleiades sample includes a half dozen stars with approximately saturated X-ray emission [$\log (L_{\rm X}/L_{\rm bol}) \sim -3$] and none of them have detected IR excesses, while our three detected sources have $\log (L_{\rm X}/L_{\rm bol}) \sim -4.2$ or less. The links between stellar mass, X-rays, and mid-IR excess in our sample are the same as in the Chen et al. (2005) sample, so selection effects may equally well explain the apparent correlation between X-ray activity and mid-IR excess. In order to draw any statistically significant conclusions we simply need larger samples and, if possible, better 70 μm limits. The lack of any *strong* correlations between other observables and debris disk detection in some sense favors a model in which the detected stars just happen to be the ones with the more recent, large collisional events, as predicted by Kenyon & Bromley (2004). However, the alternative hypothesis that there is simply a large range in debris disk masses amongst the Pleiades stars and our detected objects are just those with the most massive debris disks is also compatible with our data.

6. SUMMARY AND CONCLUSIONS

The *Spitzer Space Telescope* is providing the first statistical insight into debris disks and debris disk evolution around solar-type stars, in which context for our own solar system may be found. From a study of 20 solar-mass Pleiades members from the FEPS *Spitzer* Legacy program we have one probable and two possible detections of stars with flux excesses indicative of circumstellar dust. Our results suggest that the frequency of stars with debris disks in excess of $\sim$0.3 mJy (24 μm) at 100 Myr is thus $\sim$10%. We find that most of the sample has no detectable excess at *Spitzer* wavelengths with 3 σ upper limits of 0.15, 1.35, and 21 mJy at 24, 33, and 70 μm, respectively. Our results for the 100 Myr old solar-type Pleiades members studied here are roughly consistent with (but lower on average than) predictions of a heuristic model (D. Backman et al. 2005, in preparation) for the evolution of the Sun's debris disk.

The authors thank Jean-Claude Mermilliod for information related to HII 1101. We also thank the members of the MIPS DAT team (Karl Misselt, James Muzerolle, Karl Gordon, Chad

Engelbracht, Jane Morrison, and Kate Su) for allowing us to use the DAT software package, and we thank the other members of the FEPS team for their support and contributions to the overall FEPS program. The FEPS team is pleased to acknowledge financial support through NASA contracts 1224768, 1224634, and 1224566 administered by JPL.

REFERENCES

Backman, D. E., Dasgupta, A., & Stencel, R. E. 1995, ApJ, 450, L35
Backman, D. E., & Paresce, F. 1993, in Protostars and Planets, Vol. 3, ed. E. H. Levy & J. I. Lunine (Tucson: Univ. Arizona Pess), 1253
Backman, D. E., Stauffer, J. R., & Witteborn, F. C. 1991, in Bioastronomy: The Search for Extraterrestrial Life, the Exploration Broadens, ed. J. Heidmann & M. J. Klein (Berlin: Springer), 62
Barrado y Navascués, D., Stauffer, J., & Jayawardhana, R. 2004, ApJ, 614, 386
Bouvier, J., Cabrit, S., Fernandez, M., Martin, E., & Matthews, J. 1993, A&A, 272, 176
Bouvier, J., Rigaut, F., & Nadeau, D. 1997, A&A, 323, 139
Breger, M. 1987, ApJ, 319, 754
Chen, C., Jura, M., Gordon, K., & Blaylock, M. 2005, ApJ, 623, 493
Fazio, G., et al. 2004, ApJS, 154, 10
Gordon, K., et al. 2005, PASP, 117, 503
Johnson, H. L., & Iriarte, B. 1958, Lowell Obs. Bull., 4, 47
Johnson, H. L., & Mitchell, R. I. 1958, ApJ, 128, 31
Jones, B. F. 1972, ApJ, 171, L57
Kenyon, S., & Bromley, B. 2004, ApJ, 602, L133
Kim, J. S., et al. 2005, ApJ, in press (astro-ph/0506434)
Kraemer, K., et al. 2003, AJ, 126, 1423
Krishnamurthi, A., et al. 1998, ApJ, 493, 914
Levison, H. F., Thommes, E., Duncan, M. J., & Dones, L. 2004, in ASP Conf. Ser. 324, Debris Disks and the Formation of Planets, ed. L. Caroff et al. (San Francisco: ASP), 152
Lindroos, K. 1986, A&A, 156, 223
Mamajek, E., Meyer, M., & Liebert, J. 2002, AJ, 124, 1670
Marilli, E., Catalano, S., & Frasca, A. 1997, Mem. Soc. Astron. Italiana, 68, 895
Mathis, J. S., Rumpl, W., & Nordsieck, K. H. 1977, ApJ, 217, 425
Mendoza, E. E. 1967, Bol. Obs. Tonantzintla Tacubaya, 4, 149
Mermilliod, J.-C. 1981, A&A, 97, 235
Mermilliod, J.-C., Rosvick, J., Duquennoy, A., & Mayor, M. 1992, A&A, 265, 513
Messina, S. 2001, A&A, 371, 1024
Metchev, S., & Hillenbrand, L. 2004, Mem. Soc. Astron. Italiana, 73, 23
Meyer, M. R., & Beckwith, S. V. W. 2000, in *ISO* Surveys of a Dusty Universe, ed. D. Lemke, M. Stickel, & K. Wilke (Berlin: Springer), 341
Meyer, M. R., et al. 2004, ApJS, 154, 422
Meynet, G., Mermilliod, J.-C., & Maeder, A. 1993, A&AS, 98, 477
Micela, G., et al. 1999, A&A, 341, 751
Morbidelli, A., Levison, H., Tsiganis, K., & Gomes, R. 2005, Nature, 435, 462
Munari, U., et al. 2004, A&A, 418, L31
Pan, X., Shao, M., & Kulkarni, S. 2004, Nature, 427, 326
Papovich, C., et al. 2004, ApJS, 154, 70
Percival, S. M., Salaris, M., & Groenewegen, M. A. T. 2005, A&A, 429, 887
Preibisch, T., Guenther, E., & Zinnecker, H. 2001, AJ, 121, 1040
Prosser, C., et al. 1993, PASP, 105, 1407
Queloz, D., Allain, S., Mermilliod, J.-C., Bouvier, J., & Mayor, M. 1998, A&A, 335, 183
Raboud, D., & Mermilliod, J.-C. 1998, A&A, 329, 101
Schneider, G., & Stobie, E. 2002, in ASP Conf. Ser. 281, Astronomical Data Analysis Software and Systems XI, ed. D. A. Bohlender, D. Durand, & T. H. Handley (San Francisco: ASP), 382
Silverstone, M., et al. 2005, ApJ, submitted
Soderblom, D. R., Jones, B. R., Balachandran, S., Stauffer, J. R., Duncan, D. K., Fedele, S. B., & Hudon, J. 1993, AJ, 106, 1059
Soderblom, D. R., Nelan, E., Benedict, G. F., McArthur, B., Ramirez, I., Spiesman, W., & Jones, B. F. 2005, AJ, 129, 1616
Spangler, C., Sargent, A., Silverstone, M., Becklin, E., & Zuckerman, B. 2001, ApJ, 555, 932
Stauffer, J. R. 1984, ApJ, 280, 189
Stauffer, J. R., Caillault, J.-P., Gagne, M., Prosser, C. F., & Hartmann, L. W. 1994, ApJS, 91, 625
Stauffer, J. R., & Hartmann, L. W. 1987, ApJ, 318, 337
Stauffer, J. R., Hartmann, L. W., Prosser, C. F., Randich, S., Balachandran, S., Patten, B. M., Simon, T., & Giampapa, M. 1997, ApJ, 479, 776
Stauffer, J. R., Hartmann, L. W., Soderblom, D. R., & Burnham, N. 1984, ApJ, 280, 202
Stauffer, J. R., et al. 1999, ApJ, 527, 219
———. 2003, AJ, 126, 833
van Leeuwen, F., Alphenaar, P., & Brand, J. 1986, A&AS, 65, 309
Ventura, P., Zeppieri, A., Mazzitelli, I., & D'Antona, F. 1998, A&A, 334, 953
White, R. E. 2003, ApJS, 148, 487
Wood, B., et al. 2002, ApJ, 574, 412
Wyatt, M., Dent, W., & Greaves, J. 2003, MNRAS, 342, 876
Zwahlen, N., et al. 2004, A&A, 425, L45